PROCEEDINGS OF SCIENCE

Triangle singularity in the $J/\psi \to \phi\pi^+ a_0^-(\pi^-\eta)$, $\phi\pi^- a_0^+(\pi^+\eta)$ decays

W.H. Liang,[a,b,*] **C.W. Xiao,**[a,b,c] **J. M. Dias,**[d] **L. R. Dai**[e] **and E. Oset**[a,f]

[a] *Department of Physics, Guangxi Normal University,Guilin 541004, China*

[b] *Guangxi Key Laboratory of Nuclear Physics and Technology, Guangxi Normal University,Guilin 541004, China*

[c] *School of Physics, Central South University, Changsha 410083, China*

[d] *CAS Key Laboratory of Theoretical Physics, Institute of Theoretical Physics, Chinese Academy of Sciences,Beijing 100190, China*

[e] *School of Science, Huzhou University, Huzhou 313000, Zhejiang, China*

[f] *Departamento de Física Teórica and IFIC, Centro Mixto Universidad de Valencia-CSIC Institutos de Investigación de Paterna, Apartado 22085, 46071 Valencia, Spain*

E-mail: liangwh@gxnu.edu.cn, xiaochw@gxnu.edu.cn, jorgivan.mdias@itp.ac.cn, dailianrong@zjhu.edu.cn, Oset@ific.uv.es

We study the $J/\psi \to \phi\pi^+ a_0(980)^-(a_0^- \to \pi^-\eta)$ decay, showing that it delelops a triangle singularity at $M_{\rm inv}(\pi^+ a_0^-)$ around 1420 MeV. We evaluate the double mass distribution in terms of the $\pi^-\eta$ and $\pi^+ a_0^-$ invariant masses, observing that the $\pi^-\eta$ mass distribution exhibits the typical cusp structure of the $a_0(980)$ seen in recent high statistics experiments, and the $\pi^+ a_0^-$ spectrum shows clearly a peak around $M_{\rm inv}(\pi^+ a_0^-) = 1420$ MeV which corresponds to a triangle singularity. By integrating over the two invariant masses, we predict a branching ratio for this decay of the order of 10^{-5}, which is easily accessible in present laboratories. We also call the attention to the fact that the signal obtained is compatible with a bump experimentally observed in the $\eta\pi^+\pi^-$ mass distribution in the $J/\psi \to \phi\eta\pi^+\pi^-$ decay and encourage further analysis to extract from there the $\phi\pi^+ a_0^-$ and $\phi\pi^- a_0^+$ decay modes.

The XVIth Quark Confinement and the Hadron Spectrum Conference (QCHSC24)
19-24 August, 2024
Cairns Convention Centre, Cairns, Queensland, Australia

∗Speaker

 ISSN 1824-8039 . Published by SISSA Medialab.

PoS(QCHSC24)099

1. Introduction

Triangle singularities (TSs) were introduced in Refs. [1, 2]. As a kind of kinematic singularities,TSs can appear in processes with three on-shell intermediate particles in a triangle diagram, representing a reaction that can occur at the classical level [3]. The amplitude with a TS becomes infinite in the limit of zero widths of the intermediate particles, or turns into a finite peak when the intermediate particles have non-zero widths, simulating the behaviour of a resonance. A long list of reactions showing effects of TSs can be seen in Table 1 of the review paper [4]. Also, a reformulation of the TS has been provided in Ref. [5], which is at the same time pedagogical and practical.

The issue has emerged once more due to the recent BESIII paper [6], improving considerably on earlier measurements of the $J/\psi \to \eta\pi^0\phi$ reaction, where the ideas of Ref. [7] could be tested. Indeed, that reaction develops a TS in the $\pi^0\phi$ mass distribution, peaking around $M(\phi\pi^0) \sim 1400\,\text{MeV}$, where a clear signal is seen in Ref. [6]. Yet, the interpretation of the peak is delicate, because, as discussed in Ref. [7], the peak is masked by a tree level contribution which has also a singular behaviour. Indeed, the TS mechanism proceeds via the diagrams of Figs. 1 (a) and (b), but the same final state is reached by the tree level diagrams of Figs. 1 (c) and (d). Then, Schmid theorem [8] comes into play because if the triangle diagrams develop a TS they can be reabsorbed into the tree level diagrams with a simple change of phase, and the decay width is not affected by the TS diagrams. A thorough review of this issue was done in Ref. [9], showing that the theorem holds in the limit of the K^* width (in the present case) going to zero, and when there are no inelastic channels. The message of Ref. [9] is that all diagrams must be calculated, and that normally the tree level diagrams are mostly responsible for the mass distributions, with the effects of the TS diagrams being diluted in these distributions.

Given these problems, we look now at two related reactions where a TS develops, which is not

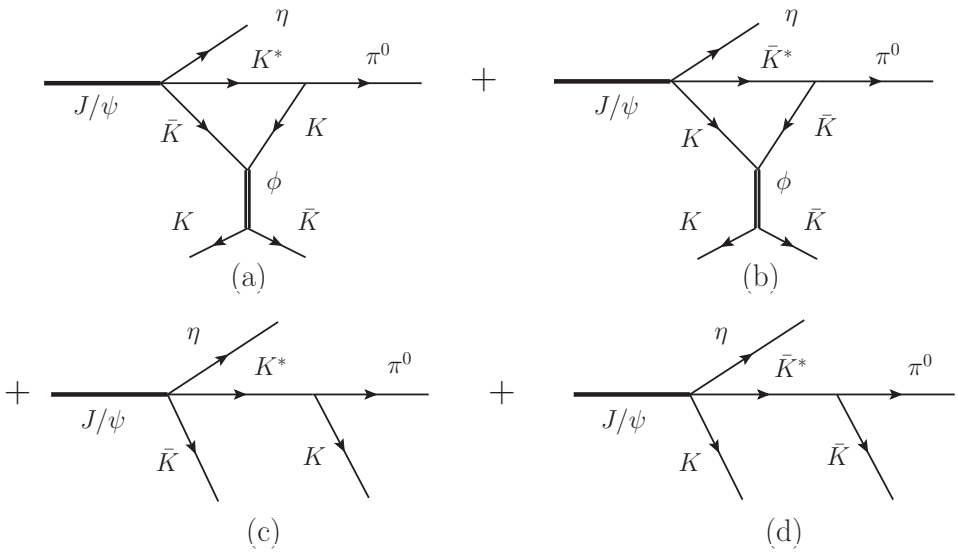

Figure 1: Mechanisms in $J/\psi \to \eta\pi^0\phi$ ($\phi \to K\bar{K}$): (a), (b) TS; (c), (d) the tree level.

masked by the effects of tree level. The reactions are $J/\psi \to \phi\pi^- a_0(980)^+(\pi^+\eta), \phi\pi^+ a_0(980)^-(\pi^-\eta)$. The mechanism for these reactions is similar to that in Figs. 1(a) and 1(b), with η replaced by ϕ, but the intermediate $K\bar{K}$ produce the $a_0(980)$ resonance which decays to $\pi\eta$. Then, the tree level diagrams with $K\bar{K}$ production do not interfere with the triangle diagram, which also develops a singularity in the $\pi a_0(980)$ mass distribution. It is easy to see where we should expect the singularity by applying Eq. (18) of Ref. [5] (with m_{a_0} slightly larger than $2\,m_K$), and one finds that a singularity should appear at $M_{\rm inv}(\pi a_0) \sim 1417$MeV. The purpose of the present work is to do a detailed study of the reaction and make a realistic prediction of the shape and size of the $\pi a_0(980)$ mass distribution in the reactions.

2. Formalism

We look at the diagrams of Fig. 2. The diagrams of Figs. 2(a) and 2(b) show the coalescence processes where the a_0^-, a_0^+ are produced, independent on the decay channel in which the a_0 resonances are observed. The diagrams of Figs. 2(c) and 2(d) show the explicit reaction, with four body final state when the $a_0^{-/+}$ decay into $\pi^{-/+}\eta$, the only sizeable decay channel. We shall consider this final state, but it is practical to consider first the coalescence processes, with only three particles in the final state. We consider the reactions $J/\psi \to \phi\pi^+ a_0^-$ and $J/\psi \to \phi\pi^- a_0^+$ as different reactions and will concentrate on the first one. The same distributions would be obtained for the second reaction.

To determine absolute rates for the $J/\psi \to \phi\pi^+ a_0^-$ ($J/\psi \to \phi\pi^- a_0^+$) reaction, we need information on the $J/\psi \to \phi K^{*+} K^-$ reaction, which we take from experiment. On the other hand,

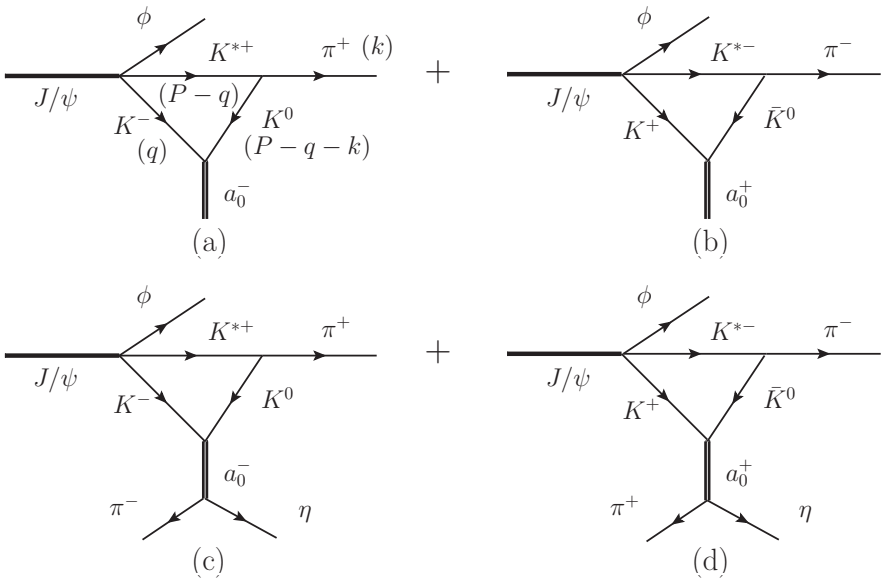

Figure 2: Triangle diagrams for $J/\psi \to \phi\pi^+ a_0^-$ decay (a) and $J/\psi \to \phi\pi^- a_0^+$ decay (b). Figs. (c) and (d) illustrate the processes of (a) and (b) respectively, with a clear depiction of the decay channel of a_0^- and a_0^+. In Fig. (a), the momenta of the particles are shown, where $P = p_{J/\psi} - p_\phi$.

the dynamics of $K^* \to K\pi$ and $K\bar{K} \to a_0 \to \pi\eta$ are well known, and for the $K\bar{K} \to a_0 \to \pi\eta$ amplitudes we shall use the chiral unitary approach [10–13].

2.1 The $J/\psi \to \phi K^* \bar{K}$ reaction

In the Particle Data Group (PDG) [14], we have the branching ratio,

$$\mathrm{Br}(J/\psi \to \phi K^*(892)\bar{K} + c.c.) = (2.18 \pm 0.23) \times 10^{-3}. \tag{1}$$

However, we are only interested in $J/\psi \to \phi K^{*-} K^+$. Using isospin and C parity arguments, it is easy to see the rate for this particular channel will be one fourth of the one in Eq. (1),

$$\mathrm{Br}(J/\psi \to \phi K^{*+} K^-) = (0.55 \pm 0.06) \times 10^{-3}. \tag{2}$$

Furthermore, the structure of the amplitude in S-wave is given by

$$t_{J/\psi,\ \phi K^{*+}K^-} = C\ \vec{\epsilon}_{J/\psi} \cdot \left(\vec{\epsilon}_\phi \times \vec{\epsilon}_{K^*}\right), \tag{3}$$

with C being a constant. We can determine C from the rate of Eq. (2) using

$$\frac{\mathrm{d}\Gamma_{J/\psi \to \phi K^{*+}K^-}}{\mathrm{d}M_{\mathrm{inv}}(K^{*+}K^-)} = \frac{1}{(2\pi)^3}\ \frac{1}{4M_{J/\psi}^2}\ p_\phi\ \tilde{p}_{K^-} \overline{\sum} \sum |t_{J/\psi,\ \phi K^{*+}K^-}|^2, \tag{4}$$

with

$$p_\phi = \frac{\lambda^{1/2}(M_{J/\psi}^2,\ M_\phi^2,\ M_{\mathrm{inv}}^2(K^{*+}K^-))}{2\,M_{J/\psi}}, \qquad \tilde{p}_{K^-} = \frac{\lambda^{1/2}(M_{\mathrm{inv}}^2(K^{*+}K^-),\ M_{K^{*+}}^2,\ M_{K^-}^2)}{2\,M_{\mathrm{inv}}(K^{*+}K^-)}, \tag{5}$$

where $\lambda(x, y, z)$ is the Källén function defined as $\lambda(x, y, z) = x^2 + y^2 + z^2 - 2xy - 2xz - 2yz$, and $\overline{\sum} \sum |t|^2$ stands for the average and sum over the polarizations of J/ψ, ϕ, and K^* mesons. Then we find

$$\frac{C^2}{\Gamma_{J/\psi}} = \frac{\mathrm{Br}(J/\psi \to \phi K^{*+}K^-)}{\displaystyle\int \frac{2}{(2\pi)^3}\ \frac{1}{4M_{J/\psi}^2}\ p_\phi\ \tilde{p}_{K^-}\ \mathrm{d}M_{\mathrm{inv}}(K^{*+}K^-)}, \tag{6}$$

from where we obtain

$$\frac{C^2}{\Gamma_{J/\psi}} = 1.381 \times 10^{-2}\ \ (\mathrm{MeV}^{-1}), \tag{7}$$

which we will use to evaluate the strength of the triangle mechanism.

2.2 The $K^* \to K\pi$ vertex and $a_0^- \to K^- K^0$ coupling

For the $K^{*+} \to K^0\pi^+$ decay, we use the Lagrangian

$$\mathcal{L} = -ig\,\langle [P,\ \partial_\mu P] V^\mu \rangle, \qquad g = \frac{M_V}{2f}, \qquad M_V = 800\,\mathrm{MeV}, \qquad f = 93\,\mathrm{MeV}, \tag{8}$$

with P and V representing the SU(3) $q\bar{q}$ matrix written in terms of pseudoscalar and vector mesons, respectively [15, 16]. The $K^{*+} \to K^0\pi^+$ vertex reads

$$-it = -ig\,\epsilon_j(K^*)\ (2k + q)^j, \tag{9}$$

which is evaluated in the frame where we take $\vec{P} = \vec{p}_{J/\psi} - \vec{p}_\phi = 0$. In this frame, we can neglect the ϵ^0 component of the K^*.

The coupling of $a_0^- \to K^- K^0$ needed in the evaluation of the diagram of Fig. 2(a) without further decay of $a_0^- \to \pi^-\eta$ can be accounted for in the following way: It is clear that if we evaluate the $J/\psi \to \phi\pi^+\pi^-\eta$ decay we would only need the $K^-K^0 \to \pi^-\eta$ amplitude. The coalescence decay $J/\psi \to \phi\pi^+ a_0^-$ should also be able to be calculated using the $K\bar{K}$ amplitudes and this is formally done as discussed below.

Assuming that, close to the peak of the $a_0(980)$,

$$t_{K^-K^0,\,K^-K^0}(M_{\rm inv}) = \frac{g^2_{a_0,\,K^-K^0}}{M^2_{\rm inv} - m^2_{a_0} + iM_{\rm inv}\Gamma_{a_0}}, \tag{10}$$

with Γ_{a_0} considered constant for the formal derivation, then, using Cauchy's integration we find immediately

$$g^2_{a_0,\,K^-K^0} = -\frac{1}{\pi}\int {\rm d}M^2_{\rm inv}\ {\rm Im}\, t_{K^-K^0,\,K^-K^0}(M_{\rm inv}). \tag{11}$$

In the coalescence process we will use Eq. (11) in the evaluation of the $|t_{\rm TS}|^2$ of the triangle diagram. We will have

$$\frac{{\rm d}\Gamma_{J/\psi,\to\phi\pi^+a_0^-}}{{\rm d}M_{\rm inv}(\pi^+a_0^-)} = \frac{1}{(2\pi)^3}\,\frac{1}{4\,M^2_{J/\psi}}\ p_\phi\ \tilde{p}_{\pi^+}\ \overline{\sum}|t_{\rm TS}|^2, \tag{12}$$

where

$$p_\phi = \frac{\lambda^{1/2}(M^2_{J/\psi},\, m^2_\phi,\, M^2_{\rm inv}(\pi^+a_0^-))}{2\,M_{J/\psi}}, \qquad \tilde{p}_{\pi^+} = \frac{\lambda^{1/2}(M^2_{\rm inv}(\pi^+a_0^-),\, m^2_{\pi^+},\, m^2_{a_0^-})}{2\,M_{\rm inv}(\pi^+a_0^-)}, \tag{13}$$

with $t_{\rm TS}$ corresponding to the amplitude for the process of Fig. 2(a). Since $|t_{\rm TS}|^2$ contains $g^2_{a_0,\,K^-K^0}$, given in Eq. (11), we can undo the ${\rm d}M^2_{\rm inv}$ integration in Eq. (12) and write

$$\begin{aligned}\frac{{\rm d}^2\Gamma_{J/\psi,\to\phi\pi^+a_0^-(\pi^-\eta)}}{{\rm d}M_{\rm inv}(\pi^-\eta)\ {\rm d}M_{\rm inv}(\pi^+a_0^-)} =& -\frac{1}{\pi}\ 2M_{\rm inv}(\pi^-\eta)\ {\rm Im}\, t_{K^-K^0,\,K^-K^0}(M_{\rm inv}(\pi^-\eta)) \\ &\times \frac{1}{(2\pi)^3}\,\frac{1}{4\,M^2_{J/\psi}}\ p_\phi\ \tilde{p}'_{\pi^+}\overline{\sum}|\tilde{t}_{\rm TS}|^2,\end{aligned} \tag{14}$$

where $\tilde{p}'_{\pi^+}$ is given by Eq. (13) substituting $m_{a_0^-}$ by $M_{\rm inv}(\pi^-\eta)$, and $|\tilde{t}_{\rm TS}|^2$ is the magnitude $|t_{\rm TS}|^2$ where we remove $g^2_{a_0,\,K^-K^0}$.

Eq. (14) can be immediately reinterpreted. Indeed, in the evaluation of $|t_{\rm TS}|^2$ for the triangle diagram of Fig. 2(c), we will need $|t_{K^-K^0,\,\pi^-\eta}|^2$ along with the extra phase space for $\pi^-\eta$ with respect to Fig. 2(a). But $|t_{K^-K^0,\,\pi^-\eta}|^2$ times the phase space for $a_0^- \to \pi^-\eta$ decay is what is given by ${\rm Im}\, t_{K^-K^0,\,K^-K^0}$ via the optical theorem. The derivation done, however, has served to go from the differential mass distribution in the three body final state to the one of the four body in a simple and intuitive way.

2.3 The triangle amplitude and the $K\bar{K}$ amplitudes

In Fig. 2(a), the K^- propagator can be written as

$$\frac{1}{q^2 - m_K^2 + i\varepsilon} = \frac{1}{2\,\omega(\vec{q}\,)} \left(\frac{1}{q^0 - \omega_K(\vec{q}\,) + i\varepsilon} - \frac{1}{q^0 + \omega_K(\vec{q}\,) - i\varepsilon} \right), \tag{15}$$

with $\omega_K(\vec{q}\,) = \sqrt{\vec{q}^{\,2} + m_K^2}$, and with q^0 positive only the first term of the former equation can go on shell, and we shall then keep this term alone. This simplifies the expression for the loop amplitude which reads, removing the $g_{a_0,\,K^-K^0}$ vertex,

$$\begin{aligned} -i\tilde{t}_{\rm TS} =& -i\,C \int \frac{\mathrm{d}^4 q}{(2\pi)^4}\, \varepsilon_{ijl}\, \epsilon_i(J/\psi)\, \epsilon_j(\phi)\, \epsilon_l(K^*)\, (-i) g\, \epsilon_m(K^*)\, (2k+q)_m \\ & \times (-i)\, \frac{1}{2\,\omega_{K^-}(\vec{q}\,)}\, \frac{1}{2\,\omega_{K^0}(\vec{q}+\vec{k}\,)}\, \frac{1}{2\,\omega_{K^{*+}}(\vec{q}\,)}\, \frac{i}{q^0 - \omega_{K^-}(\vec{q}\,) + i\varepsilon} \\ & \times \frac{i}{P^0 - q^0 - \omega_{K^{*+}}(\vec{q}\,) + i\frac{\Gamma_{K^*}}{2}}\, \frac{i}{P^0 - q^0 - k^0 - \omega_{K^0}(\vec{q}+\vec{k}\,) + i\varepsilon}, \end{aligned} \tag{16}$$

with $\omega_{K^-}(\vec{q}\,) = \sqrt{\vec{q}^{\,2} + m_K^2}$, and $\omega_{K^{*+}}(\vec{q}\,) = \sqrt{\vec{q}^{\,2} + m_{K^*}^2}$, where we have explicitly taken into account the K^* width in the K^* propagator, and P^0, k^0 are given by

$$P^0 = M_{\rm inv}(\pi^+ a_0^-), \qquad k^0 = \frac{P^{02} + m_{\pi^+}^2 - M_{\rm inv}^2(\pi^-\eta)}{2P^0}. \tag{17}$$

By summing over the K^* polarizations in the loop and integrating analytically over q^0 in Eq. (16), we obtain

$$\begin{aligned} \tilde{t}_{\rm TS} =& g\,C\,\varepsilon_{ijl}\, \epsilon_i(J/\psi)\, \epsilon_j(\phi) \int \frac{\mathrm{d}^3 q}{(2\pi)^3}\, (2k+q)_l\, \frac{1}{2\,\omega_{K^-}(\vec{q}\,)}\, \frac{1}{2\,\omega_{K^{*+}}(\vec{q}\,)}\, \frac{1}{2\,\omega_{K^0}(\vec{q}+\vec{k}\,)} \\ & \times \frac{i}{P^0 - \omega_{K^-}(\vec{q}\,) - \omega_{K^{*+}}(\vec{q}\,) + i\frac{\Gamma_{K^*}}{2}}\, \frac{i}{P^0 - k^0 - \omega_{K^-}(\vec{q}\,) - \omega_{K^0}(\vec{q}+\vec{k}\,) + i\varepsilon} \\ =& g\,C\,\epsilon_{ijl}\, \epsilon_i(J/\psi)\, \epsilon_j(\phi)\, k_l\, \tilde{t}'_{\rm TS}, \end{aligned} \tag{18}$$

with

$$\begin{aligned} \tilde{t}'_{\rm TS} =& \int \frac{\mathrm{d}^3 q}{(2\pi)^3}\, \theta(q_{max} - |\vec{q}^{\,*}|) \left(2 + \frac{\vec{q}\cdot\vec{k}}{\vec{k}^{\,2}} \right) \frac{1}{2\,\omega_{K^-}(\vec{q}\,)}\, \frac{1}{2\,\omega_{K^{*+}}(\vec{q}\,)}\, \frac{1}{2\,\omega_{K^0}(\vec{q}+\vec{k}\,)} \\ & \times \frac{i}{P^0 - \omega_{K^-}(\vec{q}\,) - \omega_{K^{*+}}(\vec{q}\,) + i\frac{\Gamma_{K^*}}{2}}\, \frac{i}{P^0 - k^0 - \omega_{K^-}(\vec{q}\,) - \omega_{K^0}(\vec{q}+\vec{k}\,) + i\varepsilon}, \end{aligned} \tag{19}$$

and

$$\overline{\sum} |\tilde{t}_{\rm TS}|^2 = \frac{2}{3}\, \vec{k}^{\,2}\, g^2\, C^2\, \left|\tilde{t}'_{\rm TS}\right|^2. \tag{20}$$

In Eq. (19) we have introduced the factor $\theta(q_{max} - |\vec{q}^{\,*}|)$, where $\vec{q}^{\,*}$ is the K^- momentum in the $\pi^-\eta$ rest frame given by [5]

$$\vec{q}^{\,*} = \left[\left(\frac{E_{a_0}}{M_{\rm inv}(\pi^-\eta)} - 1\right)\frac{\vec{q}\cdot\vec{k}}{\vec{k}^{\,2}} + \frac{q^0}{M_{\rm inv}(\pi^-\eta)}\right]\vec{k} + \vec{q}\,, \tag{21}$$

with $E_{a_0} = \sqrt{M_{\rm inv}^2 + \vec{k}^{\,2}}$, and $q^0 = \sqrt{m_K^2 + \vec{q}^{\,2}}$. This factor is demanded because in the cutoff regularization to obtain the $K\bar{K}$ scattering we have $t(\vec{q},\vec{q}\,') = t\,\theta(q_{max} - |\vec{q}\,|)\,\theta(q_{max} - |\vec{q}\,'|)$, with q_{max} the cutoff momentum used in the regularization of the $G_{K\bar{K}}$ function [17]. The value of $q_{\rm max}$ is taken from Ref. [15, 18] as $q_{\rm max} = 600\,{\rm MeV}/c$.

We use the chiral unitary approach to calculate the $t_{K^-K^0,\,K^-K^0}$ amplitude. It is extracted by solving the Bethe-Salpeter equation in coupled-channels,

$$T = [1 - VG]^{-1}V, \tag{22}$$

with V the kernel encoding the V_{ij} amplitudes from i- to j-channel. The channels considered are: $K\bar{K}$, $\pi\eta$, $\pi\pi$, and $\eta\eta$. The relevant V_{ij} amplitudes among all the channels are taken from Eq. (A.4) of Ref. [18]. Furthermore, G is a diagonal matrix with its elements G_l corresponding to the loop function for the l-th channel. We take the G_l loop function regularized by means of a cut-off $q_{\rm max}$ in the three-momentum,

$$G_l = \int_{|\vec{q}\,|<q_{\rm max}} \frac{{\rm d}^3q}{(2\pi)^3}\,\frac{\omega_1+\omega_2}{2\,\omega_1\,\omega_2}\,\frac{1}{s-(\omega_1+\omega_2)^2+i\varepsilon}. \tag{23}$$

Since, only the zero charged components are considered in Ref. [18], we make use of the fact that K^-K^0 is the $I = 1$, $I_3 = -1$ component of $K\bar{K}$ and write

$$t_{K^-K^0,\,K^-K^0} = \frac{1}{2}\left(t_{K^0\bar{K}^0,\,K^0\bar{K}^0} + t_{K^+K^-,\,K^+K^-} - 2\,t_{K^0\bar{K}^0,\,K^+K^-}\right). \tag{24}$$

3. Results and discussions

In Fig. 3, we show results for ${\rm Re}\,\tilde{t}'_{\rm TS}$, ${\rm Im}\,\tilde{t}'_{\rm TS}$ and $|\tilde{t}'_{\rm TS}|$ as a function of $M_{\rm inv}(\pi^+a_0^-)$ while fixing $M_{\rm inv}(\pi^-\eta) = m_{a_0} = 980\,{\rm MeV}$. The structure of the amplitude exhibits features typical of triangle singularities with the imaginary part peaking around the $M_{\rm inv}(\pi^+a_0^-)$, as provided by Eq. (18) of Ref. [5], and the real part changing sign around the peak of the imaginary part. It resembles much the structure of a resonance, and hence there is the danger to identify these peaks as genuine resonances, but as we can see, the origin of this structure simply comes from the triangle diagram and is exclusively tied to the combination of masses and invariant masses of the particles involved. It does not have its origin in the interaction of quarks or the interaction of hadrons. This is why it is referred to as a kinematical singularity. The modulus of this amplitude, $|\tilde{t}'_{\rm TS}|$, has a clear peak that should manifest in the studied reaction.

In Fig. 4, we show the double differential decay width normalized to the J/ψ width as a function of $M_{\rm inv}(\pi^+a_0^-)$, while fixing $M_{\rm inv}(\pi^-\eta) = m_{a_0} = 980\,{\rm MeV}$. We see a clear peak around $M_{\rm inv}(\pi^+a_0^-) = 1440\,{\rm MeV}$, coming from $|\tilde{t}'_{\rm TS}|$ in Eq. (14). This is what one would observe in a devoted experiment with a bin of 1 MeV for $M_{\rm inv}(\pi^+a_0^-)$, and 1 MeV for $M_{\rm inv}(\pi^-\eta)$.

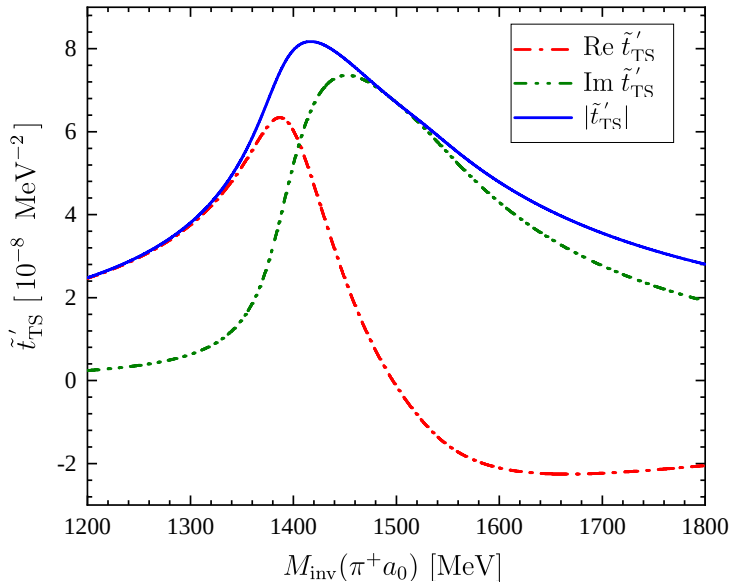

Figure 3: $\tilde{t}'_{\rm TS}$ given by Eq. (19) as a function of $M_{\rm inv}(\pi^+ a_0^-)$ when fixing $M_{\rm inv}(\pi^-\eta) = m_{a_0}$.

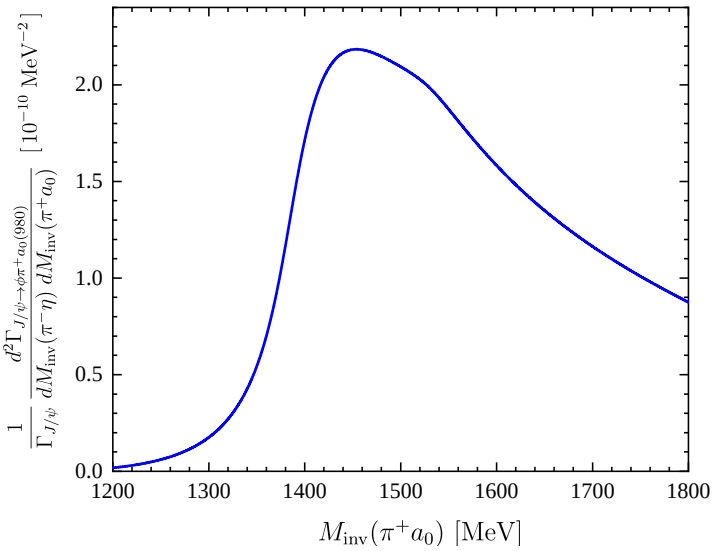

Figure 4: $\frac{1}{\Gamma_{J/\psi}} \frac{{\rm d}^2\Gamma_{J/\psi\to\phi\pi^+a_0(980)^-}}{{\rm d}M_{\rm inv}(\pi^-\eta)\, {\rm d}M_{\rm inv}(\pi^+a_0^-)}$ as a function of $M_{\rm inv}(\pi^+ a_0^-)$ when fixing $M_{\rm inv}(\pi^-\eta) = m_{a_0}$.

In Fig. 5, we set $M_{\rm inv}(\pi^+ a_0^-) = 1416$ MeV and plot $\tilde{t}'_{\rm TS}$ as a function of $M_{\rm inv}(\pi^-\eta)$. We see again that the imaginary part and the modulus delineate the shape of the $a_0(980)$ resonance. The real part changes sign at the peak of the $a_0(980)$, reflecting a typical resonance behaviour. It is interesting to see that even if the $a_0(980)$ appears as cusp, corresponding to a nearly missed bound state, or virtual state, it still exhibits the typical shape of a resonance amplitude. Such kind of behaviours for nearly missed bound states can be seen in other cases. However, there is no pole below threshold, and technically, no bound state.

In Fig. 6, we show again $\frac{1}{\Gamma_{J/\psi}} \frac{{\rm d}^2\Gamma_{J/\psi\to\phi\pi^+a_0(980)^-}}{{\rm d}M_{\rm inv}(\pi^-\eta)\, {\rm d}M_{\rm inv}(\pi^+a_0^-)}$ as a function of $M_{\rm inv}(\pi^-\eta)$, fixing now $M_{\rm inv}(\pi^+ a_0^-)$ at the peak of the TS amplitude. This comes from Eq. (14) and contains $|\tilde{t}'_{\rm TS}|^2$ along

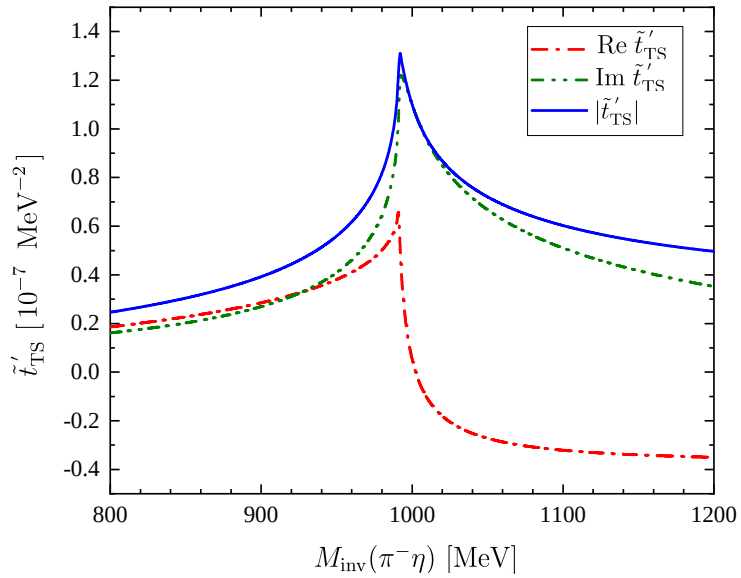

Figure 5: $\tilde{t}'_{\rm TS}$ given by Eq. (19) as a function of $M_{\rm inv}(\pi^-\eta)$ when fixing $M_{\rm inv}(\pi^+ a_0^-) = 1416\,\text{MeV}$.

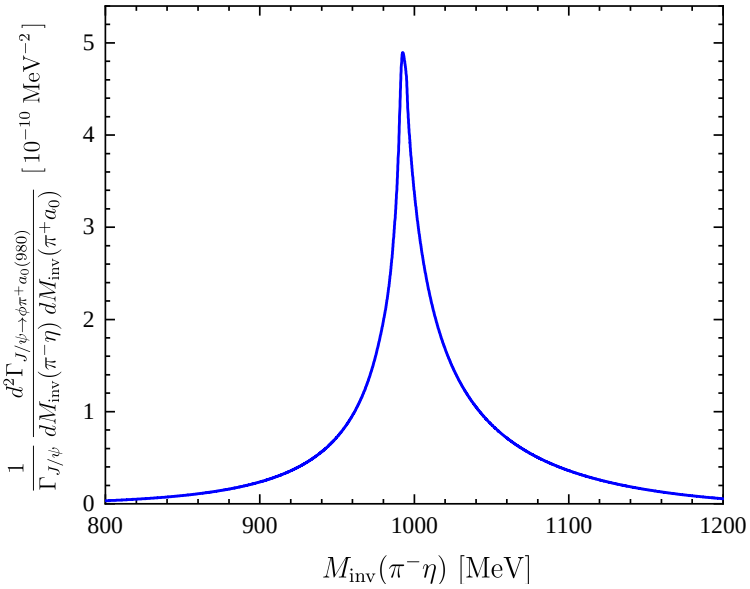

Figure 6: $\frac{1}{\Gamma_{J/\psi}} \frac{\mathrm{d}^2\Gamma_{J/\psi\to\phi\pi^+a_0(980)^-}}{\mathrm{d}M_{\rm inv}(\pi^-\eta)\,\mathrm{d}M_{\rm inv}(\pi^+a_0^-)}$ as a function of $M_{\rm inv}(\pi^-\eta)$ when fixing $M_{\rm inv}(\pi^+ a_0^-) = 1416\,\text{MeV}$.

with the phase space. The shape of the $a_0(980)$ resonance shows up as a clear cusp structure, as seen in recent experiments with high resolution [19–21].

Fig. 7 shows $\frac{1}{\Gamma_{J/\psi}} \frac{\mathrm{d}^2\Gamma_{J/\psi\to\phi\pi^+a_0(980)^-}}{\mathrm{d}M_{\rm inv}(\pi^-\eta)\,\mathrm{d}M_{\rm inv}(\pi^+a_0^-)}$ as a function of $M_{\rm inv}(\pi^+ a_0^-)$, when integrating over $M_{\rm inv}(\pi^-\eta)$ in the ranges of $m_{a_0} \pm 10\,\text{MeV}$, $m_{a_0} \pm 20\,\text{MeV}$, $m_{a_0} \pm 50\,\text{MeV}$ and $m_{a_0} \pm 100\,\text{MeV}$, respectively.

In all the cases, we observe a peak corresponding to the TS. By looking at Fig. 7, we can see that integrating the double mass distribution over $M_{\rm inv}(\pi^-\eta)$ within the range $m_{a_0} \pm 100\,\text{MeV}$ accounts for the whole strength of the $a_0(980)$ resonance, although one is introducing a bit of the $K\bar{K}$ in the final state apart from $\pi^-\eta$. We interpret these results as indicative of what should be observed in

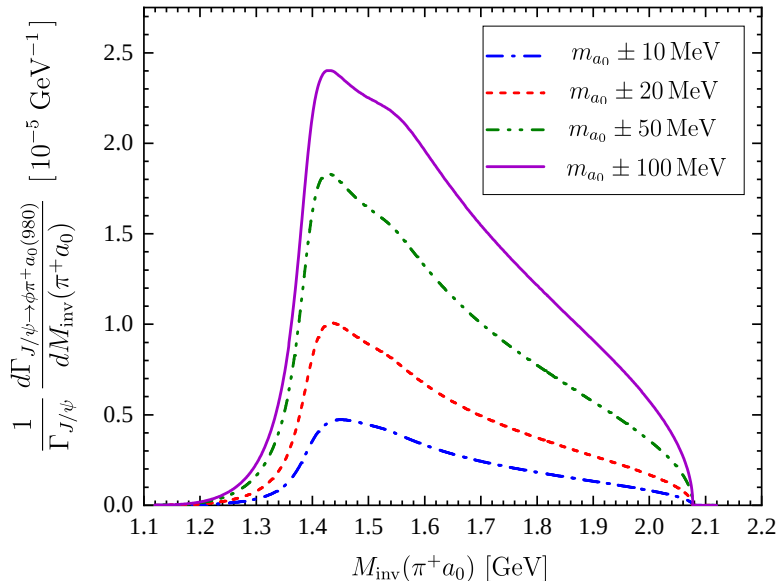

Figure 7: $\frac{1}{\Gamma_{J/\psi}} \frac{d^2\Gamma_{J/\psi\to\phi\pi^+a_0(980)^-}}{dM_{\rm inv}(\pi^-\eta)\, dM_{\rm inv}(\pi^+a_0^-)}$ as a function of $M_{\rm inv}(\pi^+a_0^-)$ when integrating over $M_{\rm inv}(\pi^-\eta)$ in the ranges: $m_{a_0} \pm 10$ MeV, $m_{a_0} \pm 20$ MeV, $m_{a_0} \pm 50$ MeV and $m_{a_0} \pm 100$ MeV.

the experiments. The shape of the TS is clearly observed.

For the case where $M_{\rm inv}(\pi^-\eta) \in [m_{a_0} - 100, m_{a_0} + 100]$ MeV, integrating over $M_{\rm inv}(\pi^+a_0^-)$ in the range $[m_{\pi^+} + m_{a_0}, M_{J/\psi} - m_\phi]$ gives the branching ratio

$$\mathrm{Br}(J/\psi \to \phi\pi^+ a_0^-) = 1.07 \times 10^{-5}, \tag{25}$$

to which we would associate an error of about 30% from the uncertainties discussed in Section 2.1 when calculating the constant C^2 and the experimental error in the branching ratio of Eq. (1) summing in quadrature. This estimate is realistic, as the only unknown magnitude required to evaluate the diagrams of Figs. 2(a) and 2(c) is the $J/\psi \to \phi K^{*+} K^-$ amplitude, which we obtained from the experimental data. This branching ratio is not small, given the copious production of J/ψ at BESIII, which allows to detect decays with branching fractions as small as 10^{-7} [14]. In view of this, we can only encourage the measurement of this reaction, which could also serve to clarify issues on the $J/\psi \to \pi^0\eta\phi\,(\phi \to K\bar{K})$ reaction [6] and its interpretation in Ref. [7] in terms of a TS. Actually, the $J/\psi \to \phi\pi^+\pi^-\eta$ reaction has already been measured at BESIII [22]. However, the mass distributions that we propose here were not investigated. Instead, the production modes of $\eta\phi f_0(980)$ and $\eta\phi f_1(1285)$ were investigated in that work.

Yet, we would like to call the attention to a feature of the reaction of Ref. [22] of relevance to our work. Indeed, in Fig. 5 of Ref. [22] there is a clear bump in the $\eta\pi^+\pi^-$ mass distribution stretching from 1400 MeV to 1530 MeV. This bump was not unnoticed in Ref. [22] and was associated to the excitation of $\eta(1405)$, which has the $\eta\pi^+\pi^-$ as one of the decay modes. In Table III of Ref. [22], the branching ratio of the bump was estimated to be $(2.01 \pm 0.58 \pm 0.82) \times 10^{-5}$. It is interesting to see that twice our rate of Eq. (25), to account also for $\phi\pi^- a_0^+$ decay, with 30% uncertainty, gives $(2.14 \pm 0.64) \times 10^{-5}$, in perfect agreement with the strength of the experimental bump. This coincidence, and the position of the peak compared to our Fig. 7 give us strong arguments to

encourage the reanalysis of this decay mode from the perspective given in the present work. Let us recall that from a resonance formation perspective, $\eta\pi^+\pi^-$ cannot be $\eta\rho^0$, which would violate isospin conservation, but can be $a_0^-\pi^+$ (the mode studied here) and $a_0^+\pi^-$ which would have the same rate of production. The study of the $J/\psi \to \phi\pi^+ a_0^- \to \phi\pi^+\pi^-\eta$ and $J/\psi \to \phi\pi^- a_0^+ \to \phi\pi^-\pi^+\eta$ decay modes would allow one to make a comparison with the predictions made here and eventually, conclude the presence of the triangle singularity discussed in this work.

4. Conclusions

We have conducted a study of the $J/\psi \to \phi\pi^+ a_0(980)^-$ $(a_0^- \to \pi^-\eta)$ decay, showing that it develops a triangle singularity at $M_{\rm inv}(\pi^+ a_0^-)$ of about 1420 MeV. The reaction proposed is motivated by the recent measurement at BESIII of the $J/\psi \to \eta\pi^0\phi$ $(\phi \to K\bar{K})$ reaction [6], that according to the work of Ref. [7] also develops a triangle singularity, however, blurred by the tree level competing mechanisms and their interconnection with Schmid theorem. In the reaction proposed, there is no tree level competing mechanism and then the TS appearing can be clearly interpreted. We evaluate the mass distributions in terms of $M_{\rm inv}(\pi^-\eta)$ and $M_{\rm inv}(\pi^+ a_0^-)$. In the $\pi^-\eta$ mass distribution we see a clear cusp structure, as observed in recent high statistics experiments, and in the $\pi^+ a_0^-$ mass distribution we observe the TS peak around $M_{\rm inv}(\pi^+ a_0^-) = 1420$ MeV. By taking information for the needed $J/\psi \to \eta K^* \bar{K}$ amplitude from experiment, we are able to determine absolute rates for the reaction. Integrating the double mass distribution in the range of the $a_0(980)$ mass and in the range of the $\pi^+ a_0^-$ mass distribution, we predict a branching ratio for the reaction of the order of 10^{-5}. Given the present rates of J/ψ production at BESIII, where branching ratios of 10^{-7} can be measured, we advocate for the measurement of these mass distributions, that apart from showing a new example of a TS can also shed light on the interpretation of the recent BESIII measurements of the $J/\psi \to \eta\pi^0\phi$ $(\phi \to K\bar{K})$ reaction. The realization of this task is more appealing since the $J/\psi \to \eta\pi^+\pi^-\phi$ reaction was already studied at BESIII [22], although the decay modes discussed here were not addressed there. We have discussed, however, that a peak seen in the $\eta\pi^+\pi^-$ mass distribution of this decay in the region 1400 – 1530 MeV is compatible with the signal that we have obtained from the TS, and encourage the experimental teams to look into the $\phi\pi^+ a_0^-$ and $\phi\pi^- a_0^+$ decay channels to further clarify this issue.

Acknowledgments

This work is partly supported by the National Natural Science Foundation of China under Grant Nos. 12365019, 11975083 and 12175066, and by the Central Government Guidance Funds for Local Scientific and Technological Development, China (No. Guike ZY22096024). This work is also supported partly by the Natural Science Foundation of Changsha under Grant No. kq2208257 and the Natural Science Foundation of Hunan province under Grant No. 2023JJ30647 and the Natural Science Foundation of Guangxi province under Grant No. 2023JJA110076 (CWX). J.M. Dias acknowledges the support from the Chinese Academy of Sciences under Grant No. XDB34030000, and No. YSBR-101; by the National Key R&D program of Chinese under Grant No. 2023YFA1606703; by NSFC under Grant No. 12125507, No. 12361141819, and No. 12047503. This project has re-

ceived funding from the European Union Horizon 2020 research and innovation programme under the program 2020-INFRAIA-2018-1, grant agreement No. 824093 of the STRONG-2020 project.

References

[1] R. Karplus, C. M. Sommerfield and E. H. Wichmann, Phys. Rev. **111**, 1187-1190 (1958).

[2] L. D. Landau, Nucl. Phys. **13**, no.1, 181-192 (1959).

[3] S. Coleman and R. E. Norton, Nuovo Cim. **38**, 438-442 (1965).

[4] F. K. Guo, X. H. Liu and S. Sakai, Prog. Part. Nucl. Phys. **112**, 103757 (2020).

[5] M. Bayar, F. Aceti, F. K. Guo and E. Oset, Phys. Rev. D **94**, no.7, 074039 (2016).

[6] M. Ablikim *et al.* [BESIII], Phys. Rev. D **110**, no.11, 112014 (2024).

[7] H. J. Jing, S. Sakai, F. K. Guo and B. S. Zou, Phys. Rev. D **100**, no.11, 114010 (2019).

[8] C. Schmid, Phys. Rev. **154**, no.5, 1363 (1967).

[9] V. R. Debastiani, S. Sakai and E. Oset, Eur. Phys. J. C **79**, no.1, 69 (2019).

[10] J. A. Oller and E. Oset, Nucl. Phys. A **620**, 438-456 (1997) [erratum: Nucl. Phys. A **652**, 407-409 (1999)].

[11] N. Kaiser, Eur. Phys. J. A **3**, 307-309 (1998).

[12] V. E. Markushin, Eur. Phys. J. A **8**, 389-399 (2000).

[13] J. Nieves and E. Ruiz Arriola, Phys. Lett. B **455**, 30-38 (1999).

[14] R. L. Workman *et al.* [Particle Data Group], PTEP **2022**, 083C01 (2022).

[15] W. H. Liang and E. Oset, Phys. Lett. B **737**, 70-74 (2014).

[16] N. Ikeno, J. M. Dias, W. H. Liang and E. Oset, Phys. Rev. D **100**, no.11, 114011 (2019).

[17] D. Gamermann, J. Nieves, E. Oset and E.R. Arriola, Phys. Rev. D **81**, 014029 (2010).

[18] J. X. Lin, J. T. Li, S. J. Jiang, W. H. Liang and E. Oset, Eur. Phys. J. C **81**, no.11, 1017 (2021).

[19] P. Rubin *et al.* [CLEO], Phys. Rev. Lett. **93**, 111801 (2004).

[20] M. Ablikim *et al.* [BESIII], Phys. Rev. D **95**, no.3, 032002 (2017).

[21] M. Ablikim *et al.* [BESIII], Phys. Rev. Lett. **132**, no.13, 131903 (2024).

[22] M. Ablikim *et al.* [BESIII], Phys. Rev. D **91**, no.5, 052017 (2015).